



A Parametric Study Of Header End-Plate Connections

Adem KARASU*¹, Haluk Emre ALÇİÇEK, Cüneyt VATANSEVER

¹Istanbul Technical University, Faculty of Civil Engineering, 34469, İstanbul

(Alınış Tarihi: 30.11.2018, Kabul Tarihi: 16.05.2019)

* İlgili yazar: karasuad@itu.edu.tr

Keywords

Steel structures
Semi-rigid connections
Header end-plate
Finite element method.

Abstract: The context of the nonlinearity provided by a building is based on the behaviors of structural components; beams, columns and their connections constituting the seismic force resisting system of the structure. Of these members, beam-to-column connections can play a considerably important role even if they have a capability of limited stiffness and flexural strength. Structural steel connections are mainly classified as a pinned or a moment connection. However, some beam-to-column connections having limited stiffness and flexural strength, which are called semi-rigid connections such as header end-plate connections can be characterized by moment-rotation relationship. For this characterization, the effect of some parameters such as thickness of the header end-plate, depth of the connection and number of the bolt rows on the behavior of header end-plate connections has been investigated by the help of finite element (FE) models. These models include material, geometrical and contact nonlinearities. Each material for each member is defined by true stress-true strain curve. According to the analyses results, in addition to shear stresses, axial tensile stresses have been observed to occur in the bolts at the tension side. Thickness of the header end-plate, depth of the connection and beam web play a governing role in the development of initial rotational stiffness and the flexural strength of the header end-plate connections. However, for the equal connection depth, increasing the number of bolt rows has not influenced the connection behavior remarkably. An additional study has also been conducted on yield line analysis to identify the behaviors of header end-plates. Analyses results have shown that header end-plate connections have limited stiffness and flexural strength. However, they seem to be promising to provide the structural systems with additional stiffness, ductility and strength.

Kısa Alın Levhalı Bulonlu Kiriş-Kolon Birleşimleri İçin Parametrik Çalışma

Anahtar Kelimeler

Çelik yapılar
Yarı-rijit birleşimler
Kısa alın levhası
Sonlu eleman modeli.

Özet: Bir binanın doğrusal olmayan davranışını deprem kuvvetini karşılayan bina taşıyıcı sistemini oluşturan kiriş, kolon ve özellikle kiriş-kolon birleşimlerinin davranışları belirlemektedir. Kiriş-kolon birleşimleri esas itibari ile mafsallı (moment aktarmayan) veya moment aktaran birleşimler olarak sınıflandırılır. Ancak, sınırlı rijitlik ve dayanıma sahip bazı kiriş-kolon birleşimleri, örneğin kısa alın levhalı yarı rijit kiriş-kolon birleşimlerinin davranışları moment-dönme eğrisi ile karakterize edilebilir. Bunun için, sonlu eleman modelleri kullanılarak alın levhasının kalınlığı ve yüksekliği ile bulon sırası sayısının moment-dönme ilişkisine etkileri araştırılmıştır. Sonlu eleman modelleri, malzeme ve geometri ile yüzey teması bakımından doğrusal olmayan davranışları içerecek şekilde hazırlanmıştır. Malzeme davranışı gerçek gerilme-şekil değiştirme ilişkisi esas alınarak tanımlanmıştır. Analiz sonuçlarına göre bulon gövdelerinde, kayma gerilmelerine ilave olarak, eksenel çekme gerilmelerinin de olduğu gözlenmektedir. Kısa alın levhalı kiriş-kolon birleşimlerinin doğrusal olmayan

davranışlarının tanımlanmasında alın levhası kalınlığı, alın levhası yüksekliği ve kiriş gövdesinin belirleyici olduğu anlaşılmaktadır. Ancak kullanılan bulon sayısı, birleşimin doğrusal olmayan davranışında belirleyici nitelikte etkin olmadığı görülmüştür. Ayrıca, alın levhalarının davranışlarının incelenmesi amacıyla, analizler sonunda bu levhalar üzerinde oluşan akma çizgileri de incelenmiştir. Analiz sonuçları, kısa alın levhalı kiriş-kolon birleşimlerinin sınırlı rijitlik ve dayanıma sahip olduğunu göstermesine rağmen, bu tür birleşimlerin yapının görece kat ötelemelerinin sınırlandırılması, enerji sönümleme kapasitesinin artırılması ve ilave bir dayanım sağlanması bakımından etkin olabileceği düşünülmektedir.

1. Introduction

Typical bolted end-plate beam-to-column connections have been studied widely over the last decades. Experimental and analytical studies showed that bolted end-plate beam-to-column connections could have sufficient rigidity, ductility and strength if designed in such a way that plastification due to plate bending has dominated the energy absorption in the connection. Also semi-rigid connections have become more popular over the years owing to ease of fabrication and erection. Moreover, these connections exhibited more suitable results than rigid welded connections (Chen et al., 2011).

Depending on the height of the end-plate, end-plate connections are classified into three main categories; extended end-plate, flush end-plate and header end-plate connections. Because of the small initial rotational stiffness, header end-plate connections fall in the category of flexible connections (Kishi et al., 2004). Also, header end-plate connections are called a shear end-plate connections in the AISC-LRFD specifications (AISC, 1994). Therefore, the studies on header end-plate connections have concentrated on experimental tests and analytical studies for achieving the moment-rotation relations (Sommer, 1969; Aggarwal, 1990; Pilgr, 2009). In the study conducted by Sommer (1969), twenty tests have been performed to observe the effects of the end-plate thickness, bolt diameter and bolt orientation on the moment-rotation relationship. Aggarwal (1990) has carried out some tests on header end-plate connections with two different end-plate configurations. Pilgr (2009) has performed experimental tests to observe the behavior of the header-end plate connections based on the moment-rotation relationship.

In this paper FE models of the header-end plate connections are presented and non-linear behavior of the connections are discussed for different end-plate configurations with three different thicknesses. The studied parameters are as follows; end-plate thickness, number of bolt rows and depth of the connection. To better understand the yield line configuration, FE analyses results have also been evaluated to observe the failure mechanisms of the connection models with different end-plate thicknesses.

2. Material and Method

In order to identify the effect of different parameters on the behavior of connection, 3-D FE models which account for both geometrical and material non-linearities are developed using the multi-purpose software package ABAQUS (Figure 1). The verification of the modelling technique was performed in the study (Karasu et al., 2018). To simulate the projected test setup, the column is assumed to be fixed at the ends and the lateral displacement of the column is prevented. A point load was applied to tip of the beam (To reference point, XRP-1 in Figure 1) which is allowed to deflect horizontally in x-direction in the same manner as in the test. The beam was laterally supported to prevent any possibility of premature failure caused by lateral torsional buckling.

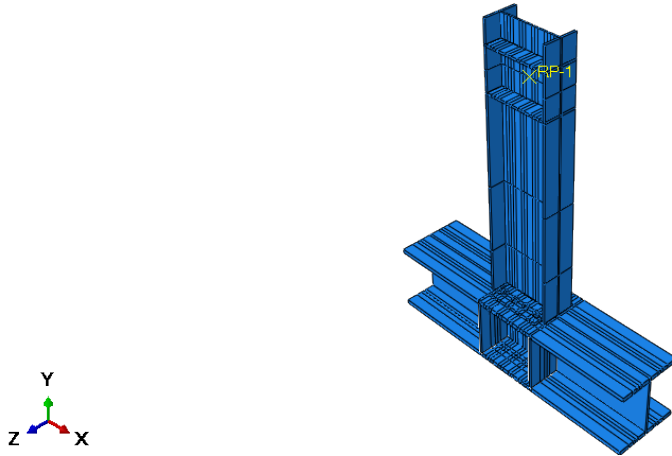


Figure 1. 3D FE model in ABAQUS (T5-15)

The specimen considered consists of a beam IPE300, end-plate with the different thicknesses of 10 mm, 15 mm and 20 mm, attached to the beam web with fillet welds and connected to the flange of the column HE300B with four, six and eight M20-10.9 bolts. All bolts are pretensioned to the minimum specified pretension force defined as 70% of the bolt tensile strength. The yield stress considered for the material of beam and column is 275 MPa (S275) and for that of the end-plate is 235 MPa (S235). To account for actual yield stress, it was increased by a factor of R_y , taken as 1.4 and 1.3 for S235 and S275, respectively. The yield and ultimate stresses of the bolts were taken as 900 MPa and 1000 MPa, respectively. Joint details are given in Figure 2. For the identification of each connection specimen, the representation of (TX-Y) is used. End-plate configuration is depicted by (TX) and end-plate thickness is denoted as (Y). For instance, T3-15 indicates that the end-plate configuration is type 3 and the thickness of the end-plate is 15 mm.

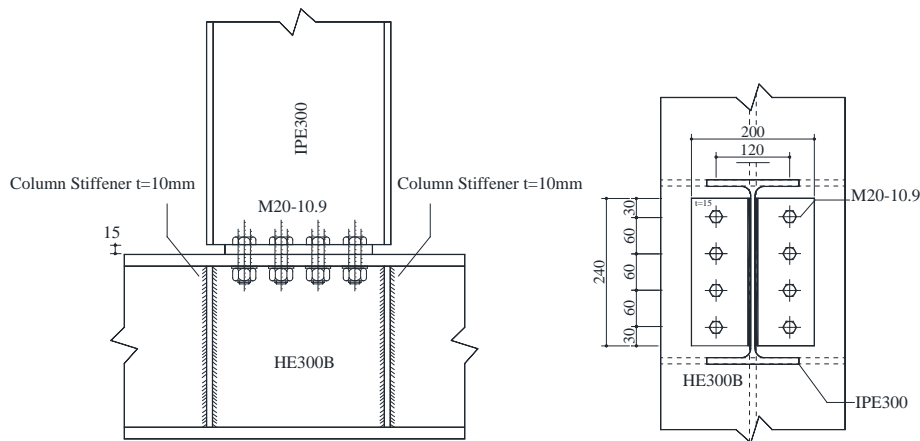


Figure 2. Details of the header end-plate connection (T5-15)

The eight-node brick elements C3D8I with incompatible modes are used. For modelling the contact interaction; between the outer surfaces of the column flange and header end-plate and between the bolt head/nut and column flange/end-plate requires two different interaction properties. First one is 'hard contact' property and the second one is tangential behavior of the contact. The friction coefficient between the contact surfaces was taken as 0.30. Also, to get acceptable results under flexural moment, at least four layers were formed through the member thickness in element meshing. The FE analyses of the model was done using two load steps. The first load step was to apply pretension forces to the bolts by applying displacements to the ends of the bolts. The prescribed bolt displacements corresponding to the axial force of 172 kN (TCDCSS, 2016) which is defined as the minimum pretension force for M20-10.9 bolts were calculated considering axial rigidity of the bolts. The second load step was employed to define monotonic loading path applied by imposing horizontal displacement to the free end of the beam.

An extensive parametric study was carried out to examine the effect of header end-plate thickness, connection depth and number of bolt rows upon the response of the header end-plate connections. The different end-plate configurations are shown in Figure 3. The thicknesses were chosen as 10 mm, 15 mm and 20 mm.

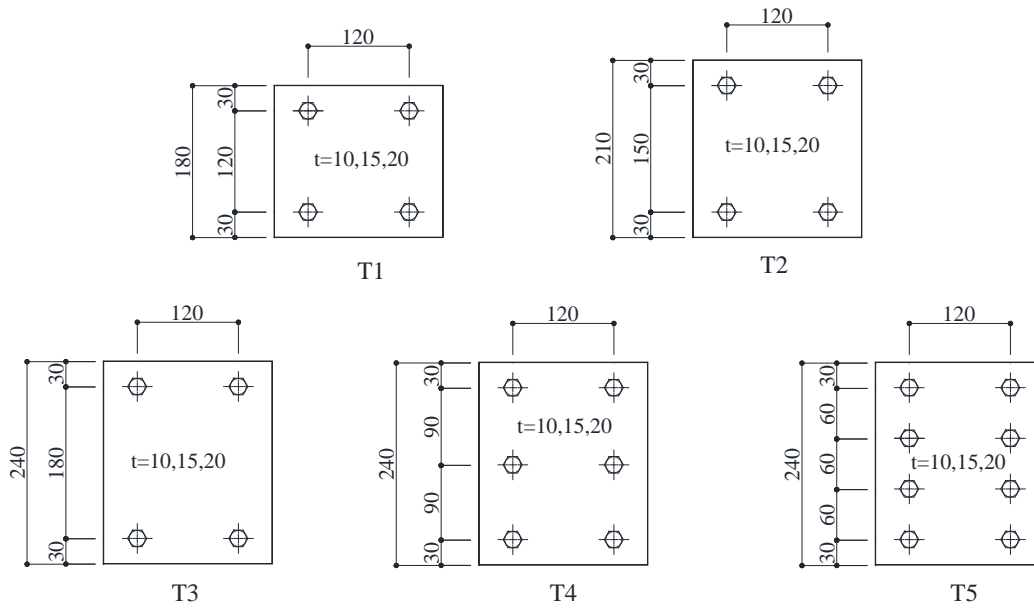


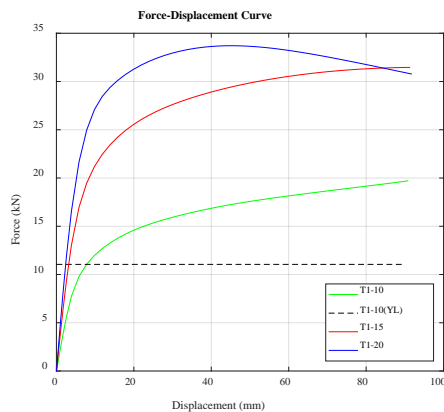
Figure 3. Different Header End-plate Configurations

3. Evaluation of Analyses Results

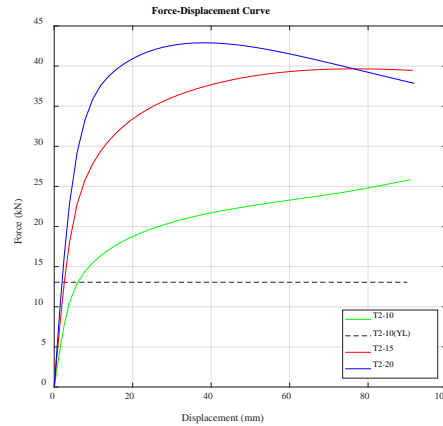
According to the analyses results from the model with thin plate configurations ($t=10\text{mm}$), the failure is governed by the end-plate flexural capacity, while in the model with intermediate plate configurations ($t=15\text{mm}$), the failure is determined by the yielding of the beam web together with the yielding of the end-plate. The post-buckling of the beam web was dominant in the others.

3.1. End-plate thickness

Figure 4 shows force-displacement curve for five different end-plate configurations with three different thicknesses. In all configurations, load carrying capacity of the joint increased by about 80% when the end-plate thickness increased from 10 mm to 15 mm since the thickness of the end-plate is dominant. However, increasing the thickness from 15 mm to 20 mm has a little effect on the capacity of the joint because the beam web post-buckling behavior is more efficient.



T1



T2

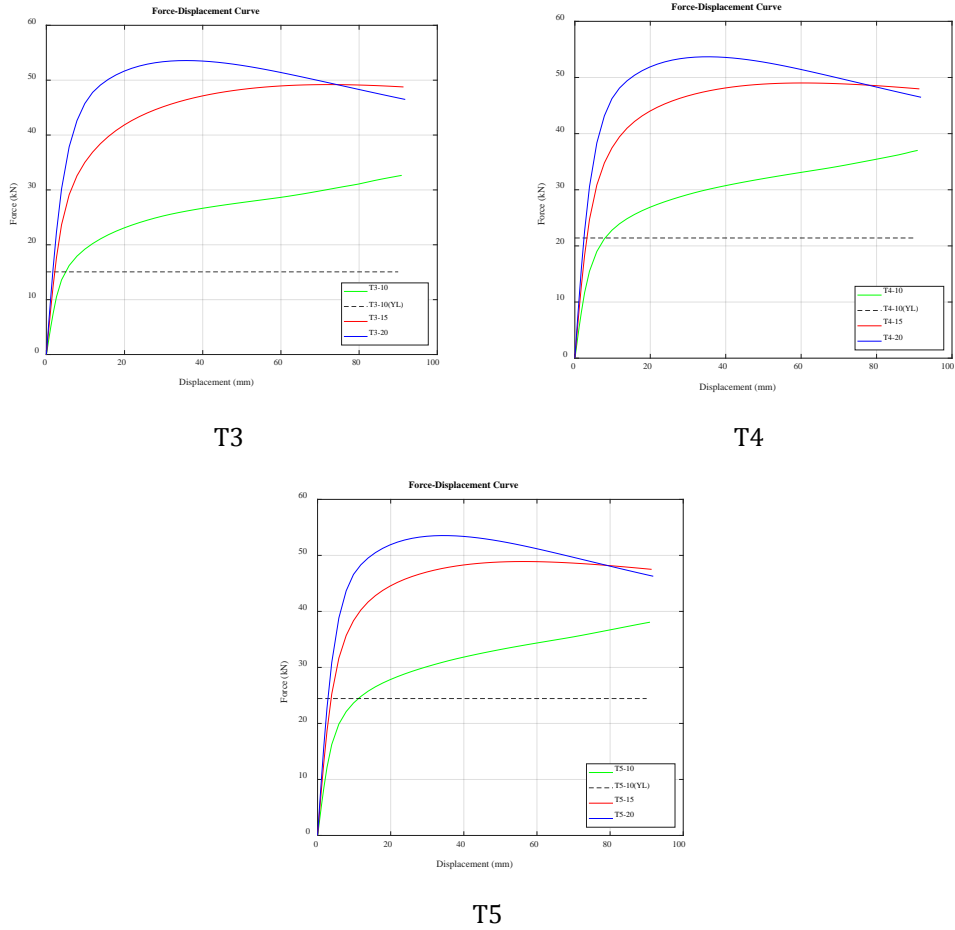


Figure 4. Force-displacement curve for different end-plate thicknesses and configurations

3.2. End-plate depth

Figure 5 shows force-displacement curves of the connections with end-plate configurations; number 1, 2 and 3 having the thickness of 15 mm. Because of the rising lever arm of the connection, the load carrying capacity of the joint increased when the depth of the end-plate increased.

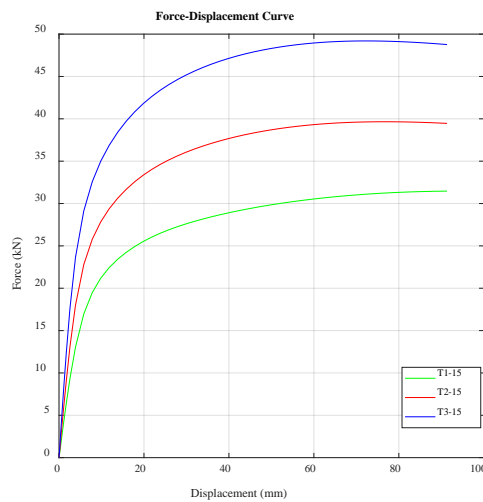


Figure 5. Force-displacement curve at different end-plate height (t=15 mm)

3.3. Number of bolt rows

Figure 6 shows force-displacement curve of the end-plate configurations; number 3, 4 and 5 with the thickness of 10 mm, 15 mm and 20 mm, respectively. The load carrying capacity of the joint increased when the number of the bolt rows increased for the end-plate with $t=10$ mm, because more bolt row provides more fixed points on the end-plate that leads to larger yielding capacity. In spite of this, effect of the number of bolt row for the end-plates with $t=15$ mm and 20 mm is found to be negligible because beam web yielding and post-buckling of the beam web govern the behavior of the joint, respectively.

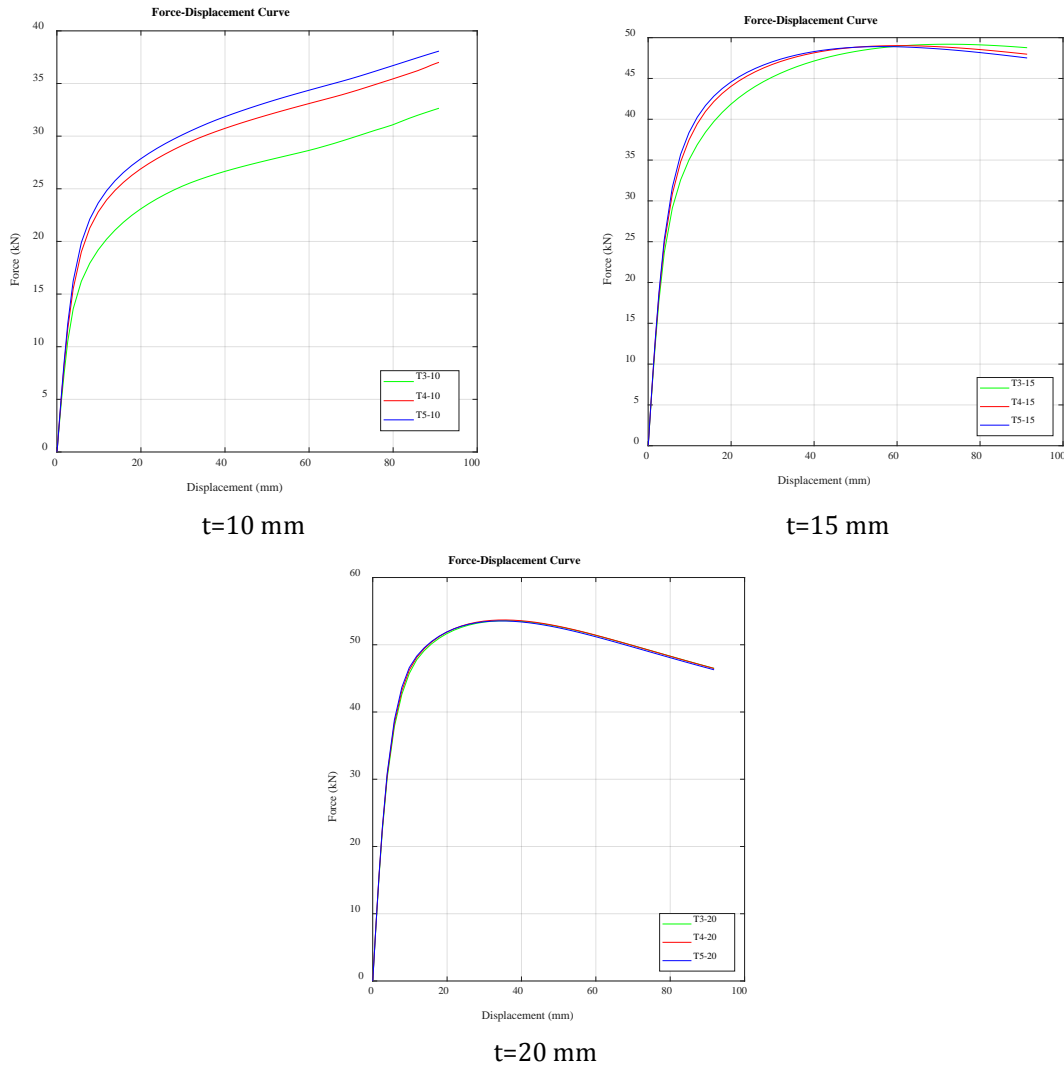


Figure 6. Force-displacement curve for equal end-plate height with different bolt row numbers

3.4. Variation of the tensile stresses in the bolts

Based on the analysis results, since the most stressed region was quarter part of the cross-section at the mid-length of the bolt shank, this region was considered to obtain the variation of axial stress. In figure 8, axial stresses were calculated by taking the average of axial stresses on the nodes within the region for the tension zone bolt row of the specimen T3-15 and T3-20. As shown in Figures 7 and 8, because the prying forces are effective, variation of axial stresses S_{22} is more noticeable for the specimen T3-15 than T3-20 in which the variation of axial stresses is obtained from tensile forces from the flexural moment of the joint only.

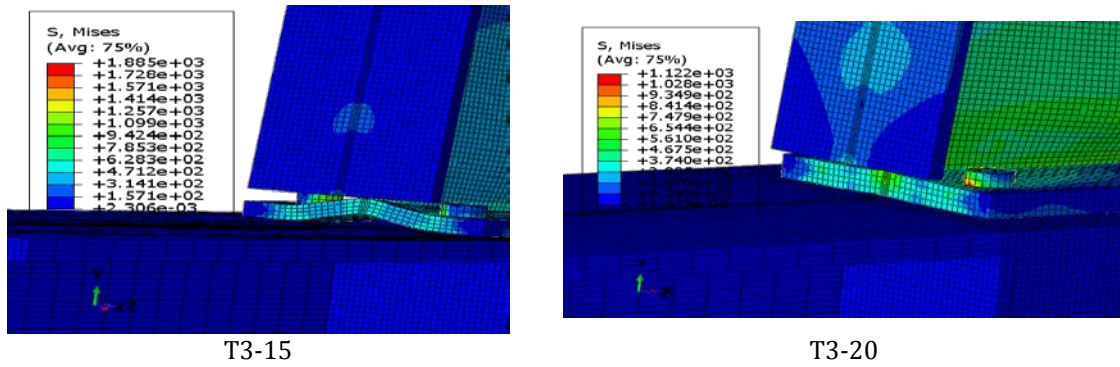


Figure 7. Stress contour diagram and deformed shape of the specimens T3-15 and T3-20

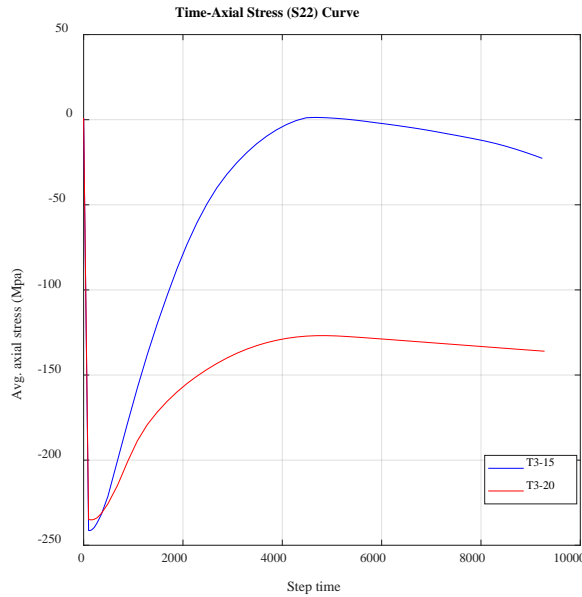


Figure 8. Variation of axial stresses S22 in the bolt shank (avg.)

3.4. Flexural resistance based on the obtained yield line configurations

In this part, end-plate flexural strength is determined using yield line analysis which estimates the yield moment of the end-plate (Bruneau et al., 2011). For this purpose, first as shown in figures 9 and 10, yield line pattern is detected and equations for internal and external work equality is generated.

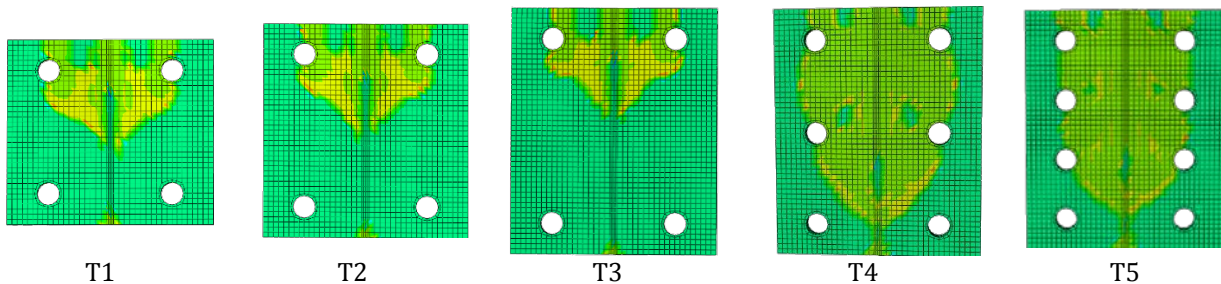


Figure 9. Observed yield line patterns for different configurations (from FE Analyses Results)

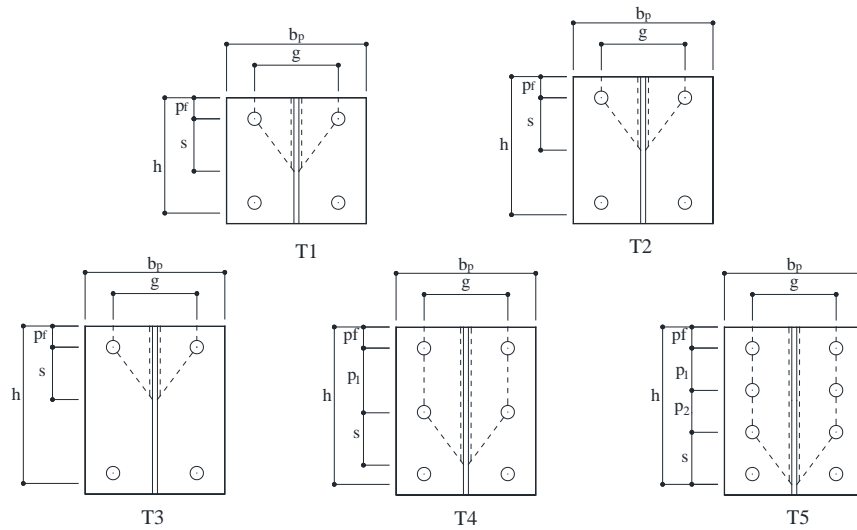


Figure 10. Assumed yield line patterns based on observation for different configurations

For simplicity, it is convenient to break the internal work components down into cartesian x and y components. General expression for internal work stored by the yield line pattern is as follows.

$$W_i = \sum_{n=1}^N (m_p \theta_{nx} l_{nx} + m_p \theta_{ny} l_{ny}) \quad (1)$$

where θ_{nx} and θ_{ny} are the x and y components of the relative rotation of the rigid plate segments along the yield line. l_{nx} and l_{ny} are the x and y components of the yield line length and m_p is the plastic moment strength of the plate per unit length which is defined as follows.

$$m_p = f_y \frac{t_p^2}{4} \quad (2)$$

t_p is the thickness of the end-plate, f_y is the expected yield strength ($1.4 \times f_y$) of end-plate material ($R_y=1.4$). For the type 1 configuration (Figure 11), the total internal work W_i stored in the yield lines can be calculated with eq 3, and external work due to bending moment M , can be calculated with eq 4. The values of p_f , g and s are 30mm, 120mm and 75 mm (from FE analyses results) respectively.

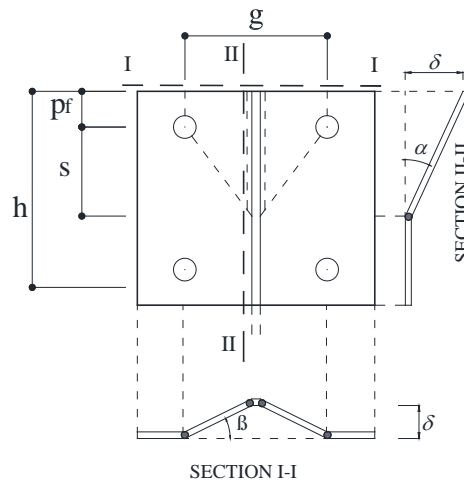


Figure 11. Yield line patterns and details of type 1 configuration

$$W_i = 2[2m_p \beta (p_f + s) + m_p \alpha (g/2)] \quad (3)$$

$$W_e = \frac{M}{h} \delta \quad (4)$$

Flexural capacity of the end-plate connections with thin plates can be calculated by yield line analysis. In the FE models the expected material properties have been taken into account while strain hardening effects has not been considered in the yield line analysis. Therefore, flexural capacities from yield line method indicates the values at the beginning of the plastification of the connection obtained by FE method as shown in Figure 4. The capacity values are given in Table 1, lever arm (h), is taken to be equal to the distance from center of the compression to the edge of the end-plate and L_{load} represents the distance between the load application point and the outerface of the column flange. Therefore, load carrying capacity of the connection is obtained by dividing the flexural capacity to L_{load} equal to 1 m.

Table 1. The load carrying capacity of the connections with thin plates

Specimen	h (mm)	m_p (Nmm/mm)	M (kNm)	$F = M / L_{load}$ (1m) (kN)
T1-10	165	8225	11.05	11.05
T2-10	195	8225	13.06	13.06
T3-10	225	8225	15.06	15.06
T4-10	225	8225	21.40	21.40
T5-10	225	8225	24.43	24.43

4. Discussion and Conclusions

A series of 3D FE analyses was conducted to investigate the behavior of header end-plate connection using a general purpose of FE software, ABAQUS. In the study, header end-plate thickness, depth of the header plate and number of bolt rows were selected as the parameters. According to the analyses results, the connections with relatively thin end-plates have reached the flexural capacity with the plastification of end-plates, intermediate end-plate connections have reached the flexural capacity with the plastification of end-plates and beam webs while the post-buckling of the beam web together with the yielding was dominant in the others. Since the post-buckling behavior of beam web causes the strength degradation, this phenomenon should be avoided. Based on the analyses results only, the ductility of the connection was found to be acceptable for thin and intermediate end-plate connections. However, an experimental research is still needed for further evaluation on the ductility.

Consequently, increasing the depth of the connection has shown enhanced capacity for all types of the end-plate configurations. End-plate thickness has significant effect on the behavior of the connection since it changes the characteristic of the connection behavior. When the number of bolt row increased, due to formation of more yield lines, load carrying capacity of the connections with thinner end plates enhanced, while this type enhancement was negligible for the connections with intermediate and thick plates. Yield line configurations, based on the FE analyses results, may be used to conservatively predict the flexural capacity of the header end-plate connections. As long as the thinner and intermediate end-plates were employed, prying forces which increase the tensile stresses in the bolts became more pronounced. However, the bolts remained elastic during the analyses. Nevertheless, based on the variation of the axial stress in bolts, it should be taken into account in the design of the bolts.

Acknowledgements

This work was supported by Research Fund of the Istanbul Technical University. Project Number: 41573

References

AISC, Load and Resistance Factor Design Specifications for Structural Steel Buildings, 2nd edition, American Institute of Steel Construction, Chicago, 1994.

Aggarwal, A.K. (1990). Behaviour of Flexible End Plate Beam-to-Column Joints. Journal of Constructional Steel Research, 16, 111-134.

Bruneau, M., Uang, C.M., Sabelli, R. (2011). *Ductile Design of Steel Structures*, second ed., McGraw Hill, New York.

Chen, W., Kishi, N., Komuro, M. (2011). *Semi-Rigid Connections Handbook*. J. Ross Publishing, U.S.A.

Karasu, A., Vatansever, C., Alçiçek, H.E. (2018). An investigation of the behavior of header end-plate connections under monotonic loading. *Challenge Journal of Structural Mechanics*, Vol. 4, No. 3 / 2018, 108-116.

Kishi, N., Komuro, M., Chen, W. (2004). Four-parameter power model for Moment-rotation curves of end-plate connections. *ECCS/AISC Workshop Connections in Steel Structures V*, (c), 99–110, Amsterdam, The Netherlands.

Pilgr, D.M. (2009). Experimental verification of actual behavior of header plate connections. *The Nordic Steel Construction Conference*.

Sommer, W.H. (1969). *Behaviour of Welded Header Plate Connections*. University of Toronto, Master's thesis, Toronto, Canada

TCDCSS (2016). *Turkish code for design and construction of steel structures 2016*, Ministry of Environment and Urbanisation, Ankara, Turkey.